Detection and Equalization of Set-Partitioned Offset-QAM OFDM in IMDD Systems

Jian Zhao, and Paul D. Townsend

***Abstract*- We design the detection algorithm for orthogonal frequency division multiplexing (OFDM) based on set-partitioned offset quadrature amplitude modulation (SP-offset-QAM) in adaptively-loaded intensity modulation and direct detection (IMDD) systems. The algorithm mitigates signal-signal beating interference (SSBI), improves the equalization capability of conventional one-tap equalizers, and reduces the complexity and the required length of training sequence in the decoding of multi-dimensional SP-QAM signals. We experimentally demonstrate adaptively-loaded SP-offset-QAM OFDM over 50-km single-mode fiber to verify the proposed algorithm. It is shown that the modified equalization significantly improves the performance while the SSBI mitigation brings benefits after transmission. The proposed decoding scheme reduces the complexity comparable to that in conventional QAM. It is also shown that SP-offset-QAM OFDM outperforms SP-based conventional QAM and conventional offset-QAM OFDM both at back-to-back and after 50-km transmission, when the algorithm is applied to all schemes.**

***Index Terms*— Orthogonal frequency division multiplexing, equalization, detection**

I. Introduction

Intensity modulation and direct detection (IMDD) systems are suitable for cost-sensitive optical access networks and data center applications. Single-carrier IMDD systems, such as carrier-less amplitude phase modulation (CAP) and pulse amplitude modulation-4 (PAM4), are preferred in high-capacity short-reach applications due to relaxed quantization resolution, device linearity [1]. However, fiber dispersion induces spectral nulls and degrades the performance for longer distances (>20 km). Multicarrier formats are more attractive in these scenarios due to their adaptive loading capability. Offset quadrature amplitude modulation (offset-QAM) orthogonal frequency division multiplexing (OFDM) is a promising multicarrier technology. In contrast to conventional OFDM which uses a sinc function with infinite spectral tails, this technology greatly relaxes the spectral profile for orthogonality and has shown advantages in super-channels, coherent transmissions, uplinks in access networks, and radio-over-fiber systems [2-6].

Manuscript received xxx. This work was supported by China "1000 Youth Talent Program" and Science Foundation Ireland grants 12/IA/1270, 12/RC/2276, and 15/CDA/3652.

Jian Zhao is with the South China University of Technology, Guangzhou, China (e-mail: zhaojian@scut.edu.cn)

Paul D. Townsend is with Tyndall National Institute and University College Cork, Lee Maltings, Cork, Ireland (e-mail: paul.townsend@tyndall.ie)

Digital Object Identifier:

On the other hand, multi-dimensional formats have been investigated in optical communication systems due to their higher power efficiency [7-9]. Four-dimensional set-partitioned (SP) PAM4 was proposed and achieved high performance and low latency in short-reach links [7]. Recently, we have proposed adaptive loading algorithm specific to SP-QAM formats and investigated SP-QAM based conventional OFDM, multi-band CAP, and offset-QAM OFDM [8]. However, these studies are based on conventional detection using one-tap equalizers. In addition, the decoding of multi-dimensional SP-QAM requires high complexity and a long training sequence (TS).

In this paper, we show that one-tap equalizers are not sufficient in IMDD SP-offset-QAM OFDM. The signal-signal beating interference (SSBI) also influences the performance after transmission due to Brillouin scattering even though this effect is negligible at back-to-back. We propose a detection algorithm for SP-offset-QAM OFDM to improve the performance and also reduce the decoding complexity. It is also shown that SP-offset-QAM OFDM outperforms conventional offset-QAM OFDM and SP-QAM based conventional OFDM, when the algorithm is applied to all schemes.

II. Principle

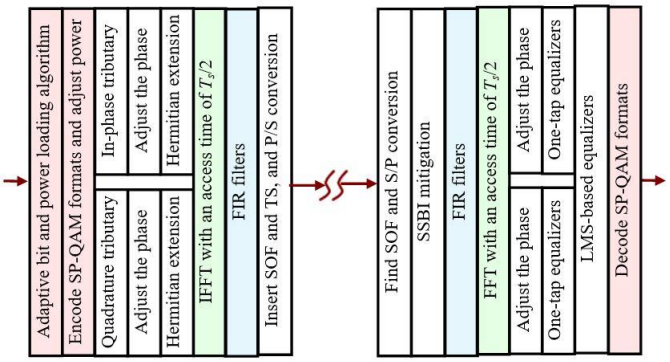

Fig. 1.Principle of SP-offset-QAM OFDM.

Fig. 1 illustrates the principle of adaptively-loaded OFDM based on the SP-offset-QAM formats. The algorithm in [8] is used to allocate bits to different subcarriers. Every two OFDM symbols of a subcarrier (denoted as Symbol #1 and Symbol #2) are encoded to generate the four-dimensional SP-QAM signal. Fig. 2 depicts the constellation of SP-8QAM and SP-512QAM as examples. We divide the constellation into two subgroups, represented by marked and unmarked circles: when the constellation point in Symbol #1 is the marked (unmarked) one,

This article has been accepted for publication in a future issue of this journal, but has not been fully edited. Content may change prior to final publication. Citation information: DOI 10.1109/LPT.2018.2883538, IEEE Photonics Technology Letters

only the point marked (unmarked) in Symbol #2 is selected. Other SP-QAM formats are derived similarly as in [8]. The data mapping of a four-dimensional SP-QAM constellation with 2^{2m-1} points can be realized as follows: the points in Symbol #1 can be encoded by m bits in the same way as in conventional 2^m QAM, while those in Symbol #2 are encoded by another m-1 bits given the mapping in Symbol #1.

The minimal Euclidean distance of SP-QAM is derived as:

$$L_{\min} = \min(L_{\text{intra}}, 2^{1/2} \times L_{\text{inter}}) \tag{1}$$

where L_{inter} and L_{intra} are the minimal distances between the two subgroups and in the same subgroup, respectively (see Fig. 2). It is readily known that $L_{\min}$ for constellations in Fig. 2 is increased by $2^{1/2}$ compared to conventional QAM.

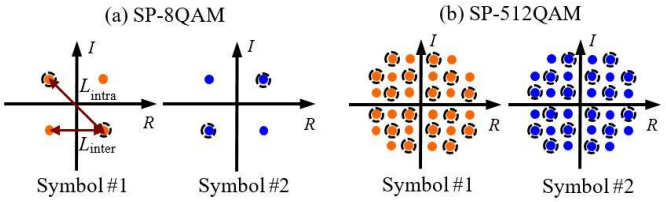

Fig. 2. Constellation of SP-8QAM and SP-512QAM. L_{inter} and L_{intra} are the minimal distances between the two subgroups and in the same subgroup, respectively.

After encoding, the quadrature tributary of each subcarrier is delayed by half a symbol period, $T_s/2$, with respect to the in-phase tributary to generate offset-QAM signals [5]. The phases of even and odd subcarriers are adjusted as in [5]. In IMDD systems, the time-domain signal should be real, which is realized via a frequency-domain Hermitian extension. A discrete Fourier transform (DFT) is used for multiplexing. The FIR filters for pulse shaping have pre-determined coefficients to create a square-root raised-cosine (SRRC) spectral profile.

At the receiver, the start-of-frame (SOF) symbol is extracted to synchronize the OFDM symbols. The signal is then serial-to-parallel (S/P) converted. In direct detection, the signal-signal beating interference (SSBI) may degrade the performance. This impairment is prominent in cases where the DC component is not large with respect to the signal. It should also be considered after transmission even though it is negligible at back-to-back, because the DC power is reduced due to the Brillouin scattering (as will be shown in the experiment). Therefore, the SSBI is firstly mitigated as follows:

$$r_i(n) = r(n) - \alpha \cdot (r_{i-1}(n) - D_{i-1})^2 \tag{2}$$

where α is a parameter to be optimized. $r(n)$ is the received signal. $r_i(n)$ is the signal after the SSBI mitigation in the i^{th} iteration and D_i is its DC component. One or two iterations are sufficient in the experiment. The FIR filters matched to those at the transmitter and an FFT are used to de-multiplex the subcarriers. The outputs include the samples at $i \cdot T_s$, targeting to decode the in-phase tributary, and those at $(i+1/2) \cdot T_s$, targeting to decode the quadrature tributary. Commonly, one-tap equalizers are used for channel equalization. The TSs can be designed as in [5] to avoid the inter-carrier interference (ICI). Note that different subcarriers are loaded with different power, which should be considered in the channel estimation and equalization. However, it is found that one-tap equalizers in this system are not as effective as in coherent systems, potentially due to the influence of the SSBI. In addition, the channel response on each subcarrier may not be flat, which would distort the SRRC spectral profile and break the orthogonality. Therefore, we propose a filter after the one-tap equalizer to re-shape the pulse. This filter benefits from the offset-QAM signal with two samples per symbol. Assuming that $b_{i,k}$ and $b_{i+1/2,k}$ are the outputs (without extraction of the real/imaginary part) from the one-tap equalizers for the i^{th} OFDM symbol and the k^{th} subcarrier, the filter coefficients (defined as $f_{n/2,k}$) are updated using the least-mean-square (LMS) algorithm:

$$b_{i',k,equ} = \sum_{n=-m}^{m} f_{n/2,k} \cdot b_{i'-n/2,k} \tag{3-1}$$

$$f_{n/2,k,updated} = f_{n/2,k} + \Delta \cdot b^*_{i'-n/2,k} \cdot \begin{cases} (\Re\{a_{i,k} - b_{i',k,equ}\}) & \text{when } i' = i \\ (\Im\{a_{i,k} - b_{i',k,equ}\}) & \text{when } i' = i + 1/2 \end{cases} \tag{3-2}$$

where m is the memory length and a number of 2~3 is able to significantly improve the performance. $\Re\{\cdot\}$ and $\Im\{\cdot\}$ represent the real and imaginary part, respectively. $a_{i,k}$ is the transmitted signal. This filter can also be applied to conventional OFDM but the filter in this case is not effective due to the single sample per symbol and the infinite spectral tails of conventional OFDM. After equalization, the in-phase and quadrature tributaries are obtained as $\Re\{b_{i,k,equ}\}$ and $\Im\{b_{i+1/2,k,equ}\}$, respectively.

Conventionally, Symbol #1 and Symbol #2 should be jointly decoded to get the SP-QAM signals in the four-dimensional constellation. In this case, the Euclidean distances between the received signal and the means of all 4-dimensional constellation points should be calculated. The decoded data is the one that gives the minimal distance. This decoding is complicated and also requires a long TS. For example, for SP-512QAM, at least thousands of OFDM symbols are required to estimate the means of all possible constellation points, and 512 distances should be compared to decode each SP-512QAM symbol. In this paper, we propose to firstly decode the two symbols individually, and find K minimal distances for each symbol (as shown later, 2~3 distances are sufficient). Then the Euclidean distances for the K^2 points in the 4-dimensional space are calculated by adding up the distances in two symbols and ranked. The K^2 points are checked as follows: when the point in Symbol #1 is the marked (or unmarked) one (see Fig. 2), the point in Symbol #2 should also be in the marked (unmarked) subgroup. The first point in the ranked order that satisfies this rule is the decoded data. This process greatly reduces the complexity and the length of the TS.

III. Experimental Setup and Results

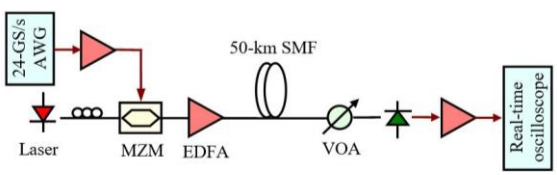

Fig. 3. Experimental setup

This article has been accepted for publication in a future issue of this journal, but has not been fully edited. Content may change prior to final publication. Citation information: DOI 10.1109/LPT.2018.2883538, IEEE Photonics Technology Letters

Fig. 3 shows the experimental setup to verify the proposed algorithm. The IFFT and FFT used 128 points, of which 63 subcarriers were modulated with SP-offset-QAM data. Another 63 subcarriers were used for frequency-domain Hermitian extension to generate a real-valued signal. The DC subcarrier was padded with zero, allowing for the insertion of bias. The SNR estimation was realized using 8QAM format. The number of allocated bits was calculated by the algorithm proposed for the SP-QAM formats [8]. The cyclic prefix (CP) was not required in offset-QAM OFDM, due to its relaxed spectral profile for subcarrier orthogonality [5]. The FIR filter created a SRRC signal spectrum with a roll-off value of 0.5. The PAPR varied by clipping and the optimal value (~ 10 dB at 50 km) that gave the best bit error rate (BER) was used for data measurement. The signal was then uploaded into an arbitrary waveform generator (AWG) with a 24-GS/s sampling rate. The bandwidth of the AWG was ~6.5 GHz. Digital pre-equalization was used to alleviate this bandwidth limitation. A laser with ~5-MHz linewidth was used to generate the optical carrier. The electrical signal was fed into a Mach-Zehnder modulator (MZM) for data modulation. The modulated optical signal was amplified by an Erbium doped fibre amplifier (EDFA) and transmitted over 50-km single mode fiber (SMF) with 10-dBm signal launch power. At the receiver, the received power was controlled at -3 dBm by a variable optical attenuator (VOA). The detected signal was electrically amplified and sampled by a 50-GS/s real-time oscilloscope. The measured number of bits was 1 million. The algorithm proposed in Section II was applied to equalize and decode the SP-offset-QAM OFDM signal. The BER was obtained by direct error counting.

Conventional OFDM was also implemented for comparison. The CP was either zero or eight samples. Other experimental parameters were the same as those in offset-QAM OFDM.

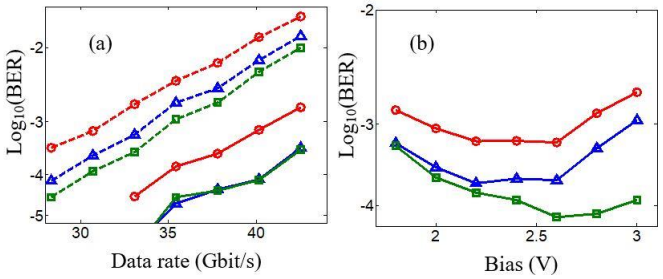

Fig. 4. (a) BER versus data rate for SP-offset-QAM OFDM at back-to-back (solid) and after 50 km (dashed). (b) BER versus the bias on the MZM at 30.7 Gbit/s and 50 km. In both figures, circles, triangles, and rectangles represent the cases without the SSBI mitigation and the equalizer (Eq. (3)), only with the equalizer, and with both SSBI mitigation and the equalizer, respectively.

Fig. 4(a) shows the performance versus the data rate for SP-offset-QAM OFDM with different algorithms. It is seen that at back-to-back, the proposed equalizer improves the performance significantly. However, the SSBI mitigation does not exhibit improvement at back-to-back, due to a sufficient DC power. After 50-km transmission, the benefit of the SSBI mitigation is observed. This is because the DC power is reduced due to the Brillouin scattering. Fig. 4(b) shows the BER versus the bias on the MZM at 50 km. It is seen that the equalizer improves the performance regardless of the bias. However, when the DC power is high (small bias voltages), the SSBI effect is small and the overall performance is degraded due to the DC power. As the DC power reduces, the influence of the SSBI increases. Without the SSBI mitigation, the performance degrades when the bias is higher than 2.6 V. On the other hand, Eq. (2) mitigates the SSBI and improves the performance.

Fig. 5(a) shows the performance versus *K*, the number of the minimal distances in each symbol used in the 4-dimensional decoding. It is seen that a number of 2-3 is sufficient to achieve the optimal performance in Fig. 5(a). Note that when K=2 is used, in a few cases in our study, none of the 4 considered points belongs to those of SP-QAM. However, K=3 works well for all results and is used throughout this paper. This reduces the decoding complexity. For SP-512QAM, the number of distance comparisons per SP-QAM symbol is reduced from 512 to 73, comparable to that in conventional QAM (64 comparisons per two symbols). Fig. 5(b) shows the BER versus the number of training symbols. This training sequence is used to estimate both the equalizer coefficients and the constellation points. It is seen that ~300 symbols can achieve the optimal performance. In contrast, when SP-512QAM is loaded in a certain subcarrier, conventional decoding requires 1000s of training symbols in that subcarrier to estimate 512 constellation points.

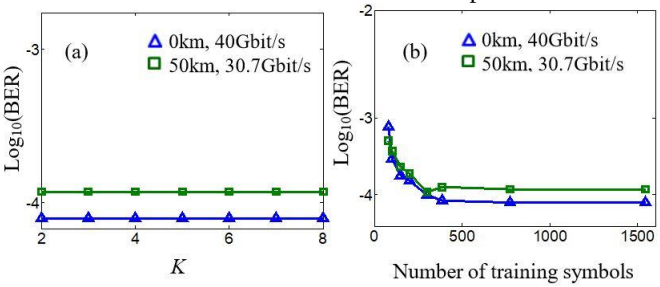

Fig. 5. (a) BER versus the number of distances in each symbol used in the 4-dimensional decoding. (b) BER versus the number of training symbols to estimate both the equalizer coefficients and the constellation points.

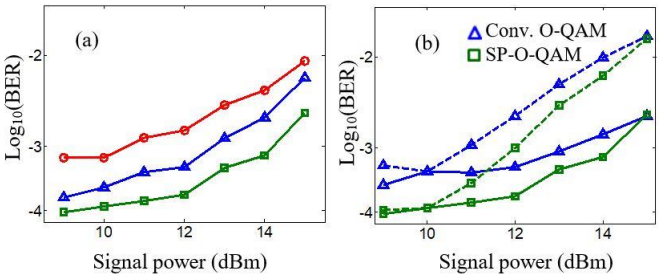

Fig. 6. (a) BER versus the signal launch power for the cases without the SSBI mitigation and the equalizer of Eq. (3) (circles), only with the equalizer (triangles), and with both SSBI mitigation and the equalizer (rectangles). (b) BER versus the launch power when the SNR estimation is performed for each power (solid) or is fixed using that obtained at 10 dBm (dashed). In both figures, the data rate is 30.7 Gbit/s and the fiber length is 50 km.

Fig. 6(a) shows the performance of SP-offset-QAM OFDM versus the launch power into the fiber. The SNR estimation and adaptive loading are performed for each power. It is seen that the benefit of the SSBI mitigation increases somewhat as the power increases. Additional results show that the output power from the fiber becomes saturated and the amplitude of the received time-domain signal becomes more unsymmetrical as the input power increases, confirming that the DC power is reduced with respect to the broadband signal for higher input powers due to Brillouin scattering. Fig. 6(b) depicts the BER

This article has been accepted for publication in a future issue of this journal, but has not been fully edited. Content may change prior to final publication. Citation information: DOI 10.1109/LPT.2018.2883538, IEEE Photonics Technology Letters

when the SNR estimation is performed either for each power or is fixed using the value at 10 dBm. Both SP-offset-QAM OFDM and conventional offset-QAM OFDM are studied. It is seen that the performance is better when the SNR is estimated for each power, resulting in more precise adaptive loading. It is also seen that SP-offset-QAM OFDM outperforms offset-QAM OFDM.

Fig. 7(a) further compares the performance of conventional offset-QAM OFDM and SP-offset-QAM OFDM. After 50-km transmission, the dispersion results in a spectral null at ~ 9 GHz as discussed in [8] and the performance is degraded compared to the back-to-back. It is shown that adaptive loading of the SP-offset-QAM formats exhibits better performance than the use of conventional offset-QAM, both at back-to-back and after transmission. This gain is prominent in the low data rate region. Fig 7(b) depicts the BER versus the roll-off factor of the SRRC function. It is confirmed that the performance of offset-QAM OFDM is not sensitive to the pulse shape, in contrast to conventional OFDM where the sinc function should be used. SP-offset-QAM OFDM outperforms the conventional offset-QAM OFDM regardless of the roll-off factor.

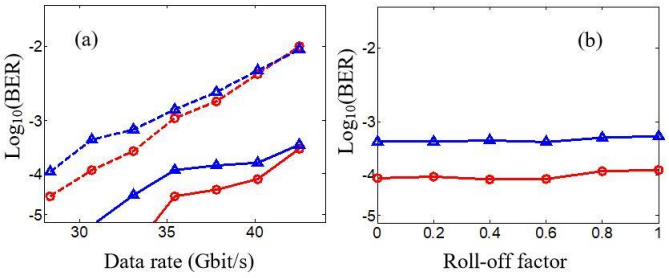

Fig. 7. (a) BER versus signal data rate at back-to-back (solid) and after 50-km transmission (dashed). (b) BER versus the roll-off factor of the SRRC function at 40 Gbit/s and 50 km. In both figures, circles and triangles represent SP-offset-QAM OFDM and conventional offset-QAM OFDM, respectively.

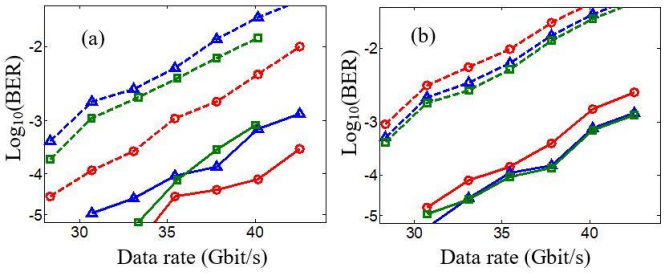

Fig. 8. (a) BER versus the data rate at back-to-back (solid) and after 50 km (dashed) for SP-offset-QAM OFDM (circles), SP-QAM conventional OFDM with the CP length of 0 (triangles) and 8 (rectangles). (b) BER versus the data rate for SP-QAM conventional OFDM at back-to-back (solid) and after 50 km (dashed). CP is not used. Circles, triangles, and rectangles represent the cases without the SSBI mitigation and the equalizer (Eq. (3)), only with the equalizer, and with both SSBI mitigation and the equalizer, respectively.

Fig. 8(a) shows the BER of SP-QAM based conventional OFDM and SP-offset-QAM OFDM. It is seen that in SP-QAM based conventional OFDM, increasing the CP length does not bring obvious benefit at back-to-back, but improves the performance after transmission. SP-offset-QAM OFDM exhibits better performance than SP-QAM based conventional OFDM at both back-to-back and after transmission, regardless of the length of CP. In order to explore the reason of this advantage, Fig. 8(b) depicts the performance of SP-QAM based conventional OFDM with different algorithms. Note that in this case, the re-shaping equalizer only has one sample per symbol. Comparison between Fig. 4(a) and Fig. 8(b) shows that SP-offset-QAM OFDM gives better performance than SP-QAM based conventional OFDM, even when SSBI mitigation and the equalizer are not used in both schemes. This might be due to the higher tolerance of offset-QAM OFDM to the loss of orthogonality by avoiding the infinite spectral tails of the sinc function. It is also seen that the equalizer in this case is not as effective as in SP-offset-QAM OFDM. It is because the equalizer only has one sample per symbol and it is also less able to obtain the sinc function than the SRRC function.

IV. Conclusions

We have proposed the detection algorithm for SP-offset-QAM OFDM in adaptively-loaded IMDD systems and verified the algorithm in 50-km SMF transmission. It is shown that this algorithm greatly improves the performance and reduces the decoding complexity, compared to the conventional algorithm. It is also shown that by using the proposed algorithm, SP-offset-QAM OFDM exhibits better performance than SP-QAM based conventional OFDM and conventional offset-QAM OFDM. The study confirms that SP-offset-QAM OFDM is a promising technology for low-cost optical access networks and data center communications.

References

[1]. K. Zhong, X. Zhou, T. Gui, L. Tao, Y. Gao, W. Chen, J. Man, L. Zeng, A. P. T. Lau, and C. Lu, "Experimental study of PAM4, CAP-16, and DMT for 100 Gb/s short reach optical transmission systems," Opt. Express vol. 23, pp. 1176-1189, 2015.

[2]. T-H Nguyen, F. Rottenberg, S-P Gorza, J. Louveaux, and F. Horlin, "Efficient chromatic dispersion compensation and carrier phase tracking for optical fiber FBMC/OQAM systems," IEEE Journal of Lightwave Technology, vol. 35, pp. 2909-2916, 2017.

[3]. Z. Li, T. Jiang, H. Li, X. Zhang, C. Li, C. Li, R. Hu, M. Luo, X. Zhang, X. Xiao, Q. Yang, and S. Yu, "Experimental demonstration of 110-Gb/s unsynchronized band-multiplexed superchannel coherent optical OFDM/OQAM system," Opt. Express, vol. 21, pp. 21924–21931, 2013.

[4]. N-Q Nhan, P. Morel, S. Azou, M. Morvan, P. Gravey, and E. Pincemin, "Sparse preamble design for polarization division multiplexed CO-OFDM/OQAM channel estimation," IEEE Journal of Lightwave Technology vol. 36, pp. 2737-2745, 2018.

[5]. J. Zhao, "Channel estimation in DFT-based offset-QAM OFDM systems," Opt. Express, vol. 22. pp. 25651-25662, 2014.

[6]. A. Saljoghei, F.A. Gutierrez, P. Perry, D. Venkitesh, R.D. Koipillai, and L.P. Barry, "Experimental comparison of FBMC and OFDM for multiple access uplink PON," IEEE Journal of Lightwave Technology, vol. 35, pp. 1595-1604, 2017.

[7]. R. R. Muller, J. Renaudier, M. A. Mestre, H. Mardoyan, A. Konczykowska, F. Jorge, B. Duval, J. Y. Dupuy, "Multi-dimension coded PAM4 signaling for 100Gb/s short reach transceivers," *Technical Digest of Optical Fiber Communication Conference (OFC)*, Paper Th1G.4, Anaheim, California USA, 2016.

[8]. J. Zhao and C.K. Chan, "Adaptively loaded SP-offset-QAM OFDM for IM/DD communication systems," Opt. Express vol. 25, pp. 21603-21618, 2017.

[9]. B. Liu, L. Zhang, and X. Xin, "Enhanced secure 4D modulation space optical multi-carrier system based on joint constellation and stokes vector scrambling," Opt. Express, vol. 26, pp. 6890-6898, 2018.

[10]. E. Giacoumidis, A. Kavatzikidis, A. Tsokanos, J. M. Tang, and I. Tomkos, "Adaptive loading algorithms for IMDD optical OFDM PON systems using directly modulated lasers," IEEE/OSA Journal of Optical Communications and Networking, vol. 4, pp. 769-778, 2012.